

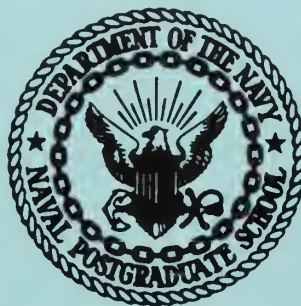
NPS ARCHIVE
1968
SLYE, R.

A FACILITY FOR TRANSIENT RADIATION EFFECTS
EXPERIMENTS AT THE NPS LINEAR ACCELERATOR

by

Richard Earl Slye
and
William Carleton Stark

UNITED STATES NAVAL POSTGRADUATE SCHOOL



THESIS

A FACILITY FOR TRANSIENT RADIATION EFFECTS
EXPERIMENTS AT THE NPS LINEAR ACCELERATOR

by

Richard Earl Slye

and

William Carleton Stark

June 1968

~~This document is subject to special export controls and each transmittal to foreign government or foreign nationals may be made only with prior approval of the U. S. Naval Postgraduate School.~~

LIBRARY
NAVAL POSTGRADUATE SCHOOL
MONTEREY, CALIF. 93940

DUDLEY KNOX LIBRARY
NAVAL POSTGRADUATE SCHOOL
MONTEREY CA 93943-5101

A FACILITY FOR TRANSIENT RADIATION EFFECTS EXPERIMENTS

AT THE NPS LINEAR ACCELERATOR


by

Richard Earl Slye
Lieutenant Commander, United States Navy
B.S., Auburn University, 1958

Submitted in partial fulfillment of the
requirements for the degree of

MASTER OF SCIENCE IN PHYSICS

and


William Carleton Stark
Lieutenant, United States Navy
B.E.E.E., Valparaiso Technical Institute, 1962

Submitted in partial fulfillment of the
requirements for the degree of

MASTER OF SCIENCE IN ELECTRICAL ENGINEERING

from the

NAVAL POSTGRADUATE SCHOOL
June 1968

NPS Archive
1968
Slye, R.

Thesis S5718
C1

ABSTRACT

Mechanical hardware has been developed that remotely places integrated circuits, transistors, and other fixed components into an electron beam in a manner which allows measurements of radiation effects. The associated circuitry used for these measurements is presented, as well as the methods employed in reducing RF noise. A technique which uses a set of cross hairs to give time and spatial beam profiles which aid linear accelerator tuning and beam manipulation is described. Initial transient radiation effects experiments have been conducted and photo currents observed. Schematics, pictures, and construction details of the apparatus are presented.

TABLE OF CONTENTS

Section		Page
I	Introduction	9
II	Elimination of Noise	13
III	Remote Positioning Equipment	15
A	Wheel	16
B	X-Y Table	19
IV	Control Station Apparatus	22
V	Dosimetry	27
A	Calculated Dose Rate from Secondary Emission Monitor Readings	27
B	X-Y Cross Hairs	29
C	Color Film Dosimeters	32
VI	Tuning the Linac Using Time Profiles of Beam Pulses	34
VII	Radiation Effects Experiments	38
VIII	Bibliography	47
IX	Appendicies	
A	Illustrations of Experimental Apparatus	48
B	Spatial Profiles of Radiation Dose	54

LIST OF ILLUSTRATIONS

Figure		Page
1	Diagram of Linear Accelerator	10
2	Block Diagram of Electrical Connections in Wheel	17
3	Hydraulic Flow Diagram of X-Y Table	20
4	Electrical Block Diagram of X-Y Table	21
5	Wiring Schematic of Table Position Indicator	23
6	End Station Control Panel	24
7	Integrated Current Profiles	31
8	Time Profile of Correctly Tuned Beam	34
9	Sequence of Time Profiles as Frequency is Raised	35
10	Time Profile with Section 3 Phasing Late	36
11	Time Profile with Section 3 Phasing Early	36
12	Time Profile with Deflection Magnet Current High	36
13	Time Profile with Deflection Magnet Current Low	36
14	Time Profile of 0.1 Microsecond Pulse	37
15	Circuit Configurations for Exposing Transistors	38
16	Isolated Component Circuit Configurations and Waveforms	41
17	Block Wiring Diagram for Logic State Experiment	44
18	Logic Circuit Output without Emitter Follower	44
19	Logic Circuit Output with Emitter Follower	45
20	Transfer Characteristics of a Logic Circuit	46
Appendix A		
1	Wheel Disc	48
2	Wheel Assembly	49

		Page
3	Wheel Assembly Showing X-Y Cross Hairs	50
4	X-Y Table	51
5	Control Panels	52
6	Diagram Identifying Control Panel Components	53

ACKNOWLEDGEMENTS

The authors wish to express their appreciation to Professors John Dyer, William Brenner, and Shu-gar Chan for their interest and assistance in all phases of the research. Acknowledgements are also extended to Professor Franz Bumiller for the use of the linear accelerator and many discussions concerning its operation, and to Professor Fred Buskirk for the development of the Linac single pulser. The efforts of Mr. Michael O'Day for his contributions to the building of positioning equipment are gratefully noted.

Special mention is made of Fairchild Semiconductor a division of Fairchild Camera and Instrument Corporation for providing the integrated circuits and to the Naval Radiological Defense Laboratory for aiding in dosimetry and providing a densitometer for the project.

I. INTRODUCTION

The primary aims of this thesis are to describe the design and construction of the apparatus needed to measure transient radiation effects in microelectronics and to report the results of preliminary investigations of electron beam dosimetry. Initial results of radiation effects experiments which serve to test the new equipment are also reported.

Initial radiation damage research conducted last year by J. H. Brady¹ and early findings of this project indicated the need for electromagnetic noise reduction, automation in circuit positioning, and improved techniques in the control and measurement of the electron beam.

The project was an outgrowth of the availability of the NPS electron linear accelerator². The accelerator, which became fully operational in the latter part of 1966, is diagramed in Fig. 1. It consists of three ten-foot sections each powered by a klystron that delivers up to 22 megawatts of peak power. For this project, it was operated generally at an energy of about 80 million electron volts (MeV) with a pulse repetition frequency of 60 pulses per second and a pulse duration of either one-half or one microsecond. The average current was three microamperes, which produced a dose rate in silicon of approximately 10^{10} rads.

A primary hinderence to Brady was the excess of electromagnetic noise. An investigation subsequent to his work showed the noise to be so severe as to render inconclusive any indication of the photo currents he reported. It now is believed that these reported

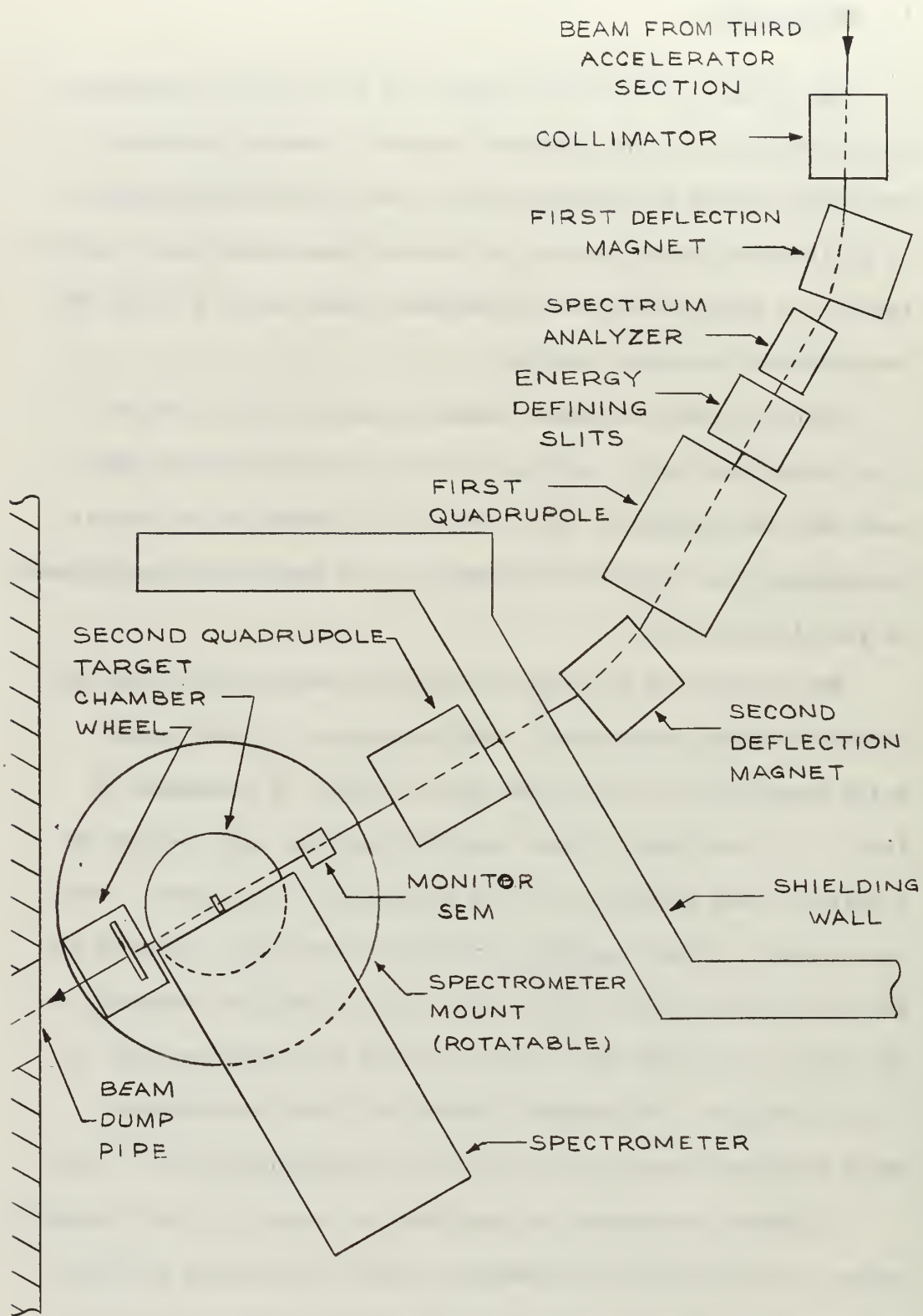


Figure 1. Diagram of Linear Accelerator

photo currents were noise picked up in connecting cables. Therefore, the first concern of this project was the elimination of noise.

Before measuring transient radiation effects it was necessary to develop the capability to position and reposition various integrated circuits in the same portion of the electron beam. Thus, of secondary concern was the fabrication of remotely controlled positioning equipment which would precisely locate devices and which would transmit any signals or effects that might originate in the irradiated circuits. Associated equipment to monitor these signals, various power supplies, signal generators, and controlling panels had to be constructed or procured and organized in a manner such that experiments might be conducted efficiently and economically.

A third objective was to develop beam handling techniques which would increase the radiation dose rate and to measure accurately this rate at the position of the circuit.

Finally, it was desired to conduct certain transient radiation effects experiments on integrated circuits, qualitatively observing photo currents or other effects that might appear, under a range of input and biasing parameters. The circuits chosen were Fairchild Integrated Circuits DTuL-962 and DTuL-969, which are identical except for the latter being dielectrically isolated and containing thin film resistors.

Fairchild fabricated some conventional DTuL-969 circuits in which the final interconnection wiring mask was eliminated. Eight of the circuit's transistors and two fixed resistors were brought out to the terminals of the dual in line package. Normal packaging

was then completed. This configuration allows observation of the radiation effects on one isolated transistor or resistor that normally is a component of a complete logic circuit.

At present the first two objectives have been met. RF noise has been reduced to a tolerable level. All positioning hardware has been built and other experimental apparatus assembled and tested. To aid in certain measurements the Linac has been modified to include single pulsing.

Improved beam control has increased the dose rate from 10^8 to 10^{10} rads per second during the past year. Satisfactory dosimetry, however, has not been achieved. Under conditions of optimum Linac tuning the dose rate can be calculated from the integrated current of a calibrated secondary emission monitor, provided the beam size and electron distribution are known. These are not usually known with great accuracy.

Photo currents in transistors have now been observed. It is anticipated that future investigations will result in quantitative measurements of these photo currents and in development of a model on the basis of the data obtained. In order to measure the same phenomena in integrated circuits, additional work should be directed toward narrowing the pulse width of the beam without lessening the dose rate.

II. ELIMINATION OF NOISE

The final solution of the electromagnetic noise problem was surprisingly simple, although not anticipated. It consisted primarily of heavily shielding all components between the target and the monitoring equipment. The resultant noise level was reduced to less than 1 millivolt, a decrease of approximately 43 db from that reported by Brady.

The noise ranged in frequency from 1 to 100 megacycles and its magnitude was excessive with respect to the anticipated photo current. It occurred a few microseconds prior to and subsequent to the pulse arrival but was absent otherwise. The steps taken to solve the noise problem are presented below.

An attempt was made to eliminate the manner in which the noise was injected into the monitoring system. Nine runs of RG-58A triaxial cable were strung from the Linac control station to the target station in a cable tray separate from the main Linac cable tray containing the Linac trigger pulse and RF lines. The new cable tray came no closer than ten feet to the Linac tray. Special constant impedance UG-88C 50 ohm BNC connectors were connected to the new cables. These connectors were chosen to minimize an impedance mismatch that could result from connections in the target and control stations. A small aluminum box grounded to a water pipe enclosed an integrated circuit used for the operational noise evaluation. To ground the system further and remove any chance of a floating system, holes were drilled in the concrete floor of the building at both the Linac control station

and at the radiation damage monitoring station. Three-quarter inch copper rods were sunk five feet into wet earth. The Linac control station was grounded to one rod; the radiation damage monitoring equipment to the other. With these measures the noise remained excessive. Standard methods of shielding and grounding failed to reduce the level. Various schemes which did not prove to be effective included commonly grounding the target shield and the outer triaxial shield with the Linac system ground.

By observing the change in noise level when turning the machine on and off it was determined that the electron beam, the grid circuits, and the power supplies to the electron gun contributed very little to the noise. The primary source appeared to be the 1,500 volt power supply for the triggering system. This suggested the need for additional shielding.

It was noted in a trial and error process that the noise could be eliminated by completely enclosing a section of triaxial cable in conduit pipe. As little as two inches of this cable outside of the conduit pipe in the monitoring area was a sufficient antenna to pick up nearly 100 per cent of the original noise. After these findings, all triaxial cables were placed in conduit pipe. All exposed cables coming from the pipe at the target station and control station were enclosed in a thick copper braid. The braid was connected to the conduit pipe and the BNC connectors, thus making common the pipe, braid, aluminum box and the two shields of the triaxial cables. This scheme reduced the noise to the level reported.

III. REMOTE POSITIONING EQUIPMENT

The Fairchild integrated circuits used in these experiments present a target small compared to the beam size. To obtain reliable measurements it was necessary, therefore, to develop the capability to place the integrated circuits in that portion of the beam in which the electron flux is greatest. This required the design of a remotely controlled device which could consistently position circuits with an accuracy of about one millimeter. Although it is possible to steer the electron beam by means of steering coils and quadrupole magnets, it was found that this sometimes diffused the beam and gave a nonsymmetric beam profile which both lowered the radiation dose rate and radically changed the rate from point to point within the profile. To position the device manually with the beam off presented the problem of not knowing the exact beam location. Furthermore, the trial and error positioning method of frequently turning the beam off in order to adjust the position of the device is a waste of Linac running time. Thus, it was necessary to construct positioning equipment that met the following criteria:

1. The capability to move the device in the X-Y plane (i.e., the plane perpendicular to the incident electron beam) slowly and accurately, and to provide remote indication of position.
2. The ability to move successively several devices into the beam at the same position without having to enter the target station.
3. The provision of sufficient shielding to prevent the introduction of unwanted electromagnetic noise.

4. The capability to measure the beam intensity immediately behind the device so that dosimetric information would be constantly available on a pulse to pulse basis as required for single pulse transient measurements.
5. The ability to verify that the equipment is completely aligned (i.e., ensuring that the electron beam, integrated circuit and the measurer of radiation dose lie on the same line).

A. WHEEL

To satisfy these criteria (except the first) a mechanical positioning apparatus was constructed which hereafter will be referred to as the wheel. A similar device used in radiation effects experiments was first observed at General Atomics, a division of General Dynamics Corporation. More recently the Army Electronics Command³ described a wheel which is in many ways similar to the device used in this research. As shown in Fig. 1 of Appendix A, a circular disc onto which are mounted the various integrated circuit sockets, associated circuitry, and hardware is used. Such a design allows each integrated circuit to be placed in the proper position. To connect a series of input-output, bias, and monitoring cables to the integrated circuit without interrupting operation of the wheel, two C. P. Clare RP 10945G3 relays were chosen. These employ gold contacts to minimize contact resistance, are hermetically sealed and can accommodate eleven IC configurations. RG 174 50 ohm mini-coaxial cable is used for all connections between the sockets and the relays and between the relays and the wheel input-output terminals to match impedances as well as possible and to keep the

noise level at a minimum. Thus, by cycling the relay, the circuit of choice can be connected to a single set of cables that run to the monitoring area. Two sections of the relay are used to operate a two digit decimal nixie tube display which indicates the circuit which is connected to the monitoring equipment. The energizing coils of the relays are connected in parallel through a push button to a 24 volt power supply. Figure 2 is a diagram of the wiring.

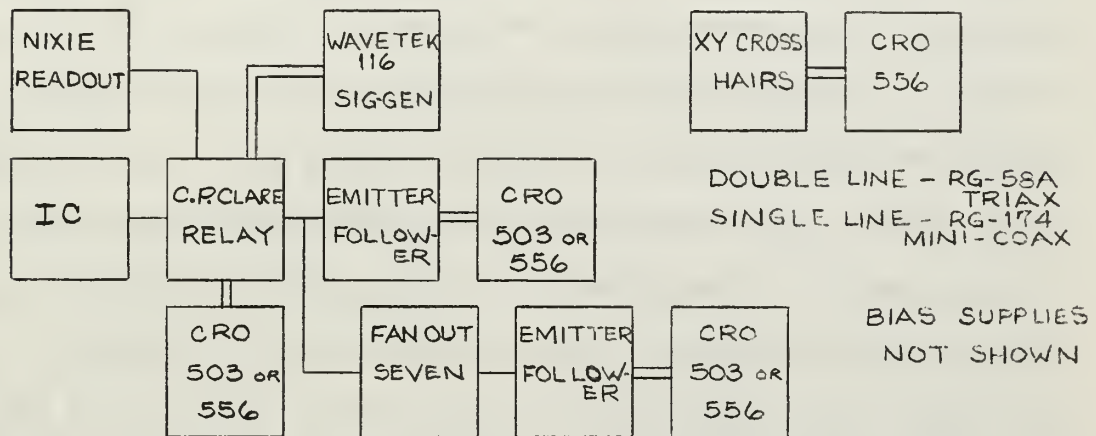


Figure 2. Block Diagram of Electrical Connections in Wheel

The wheel disc has three types of sockets which allow flexibility in circuit testing.

- a. Three sockets for flat-paks (AUGAT 8075)
- b. Two sockets for T05 or T018 cans (AUGAT 8058)
- c. Six sockets for 14 pin dual in line circuits (AUGAT 8135)

The disc is wired to accommodate a normal 962/969 logic circuit.

The ground used in this circuit is a floating connection to a series of BNC output connectors on the assembly casing. When using a logic configuration the ground isolated terminal is shorted with a BNC shorting connector to the casing and thus to the common ground for the entire monitoring system. When using isolated

components of a circuit or transistors the ground isolated terminal is used as a conventional terminal point.

A method was needed to indicate when a given circuit was precisely rotated into position. The manner in which the circuit is placed horizontally or vertically into the center of the beam will be discussed subsequently. For correct centering, a photo diode assembly was incorporated into the wheel design as shown in Fig. 2 of Appendix A. The photo diode is fixed on a stationery portion of the structure that lies on the centerline of the wheel assembly. Also mounted on the centerline separated by the outer portion of the wheel disc is a 24 volt light bulb used as the photo power source. At the same distance from wheel center along each radial line that passes through a circuit, a .015 inch hole is drilled through the disc. Thus, when the circuit is correctly positioned, light from the bulb travels through the hole into the photo diode. The light causes the photo diode to conduct and the current is registered on a control panel meter in the monitoring area. The wheel disc can be rotated for maximum meter deflection.

Horizontal and vertical cross hairs are fixed into position on the centerline of the wheel structure. As the disc turns, the cross hairs clear between the circuit and the disc as is shown in Fig. 3 of Appendix A. When the circuit is in position the center of the cross hairs lies directly behind the circuit. The main purposes of the cross hairs are for beam profiles, alignment of the wheel, and dosimetry.

Before an experiment each integrated circuit is aligned by positioning the disc for maximum photo diode current and setting each socket by means of set screws so that the integrated circuit is centered in front of the cross hairs.

To prevent the wheel assembly from having antenna characteristics and picking up the unwanted electromagnetic noise discussed previously, the entire system is enclosed in three-eighths inch aluminum plate. Monitoring, power, and nixie cables are introduced at the lower portion of one side. One and one-half inch diameter holes are cut out of the front and back of the assembly for the electron beam. Only a slight increase of noise was noticed between terminated shielded cable and the attachment of this cable to the enclosed wheel. The increase can be attributed to extraneous RF pick up, non-collimated electrons producing gamma rays when striking the outer shielding, or the ionized air produced by the passing beam.

To prevent noise which originally was introduced into the enclosure by the unshielded power and Nixie cables, a 0.1 microfarad mica capacitor is placed between each Nixie lead and ground and a 1.0 microfarad capacitor is placed between the negative Nixie common and ground. The 24 volt power cable is bypassed to ground by a 0.1 microfarad capacitor.

B. X-Y TABLE

The entire wheel assembly rests on a table which is remotely movable in the X-Y plane. Three major factors had to be met in its design. First, the table had to be slow moving so that it could be precisely positioned. Second, it had to have a range of movement which would carry circuits in and out of the beam in the

X-Y directions. Finally, the table had to be designed to lift 80 pounds without pitching or yawing. A pilot design using a threaded drive to converge the cross members between two scissors did not meet the last criterion and indicated the need for a hydraulic lifting mechanism.

The present design shown in Fig. 4 of Appendix A uses a 30 volt dc motor to drive a hydraulic counter-rotating gear pump for vertical movement. Oil is drawn from a reservoir through the pump to the bottom of the piston at a rate that lifts or lowers the table approximately four inches per minute. Figure 3 shows a schematic of the

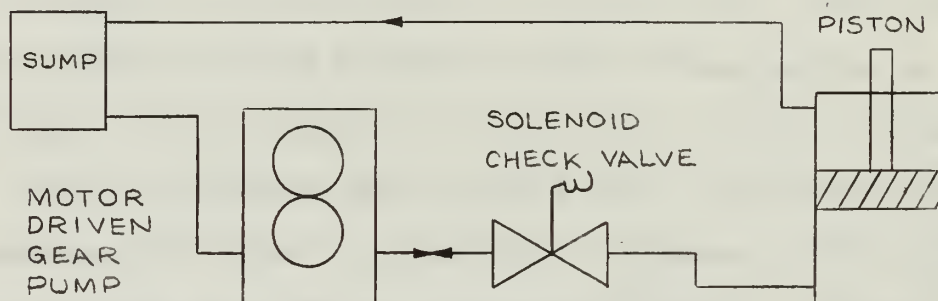


Figure 3. Hydraulic Flow Diagram of X-Y Table

hydraulic flow. A solenoid controlled check valve prevents gradual dropping of the table due to oil seepage through the gear pump. Limit switches allow vertical travel of $2\frac{1}{2}$ inches. The table top consists of two parallel plates held together by rods that allow lateral movement. A motor driven threaded rod moves the upper plate relative to the fastened lower plate at a rate of one inch per minute. Four inches of horizontal travel are allowed.

The horizontal and vertical positions are measured by two Bourns Model 108 linear potentiometers. These are indicated by arrows in Fig. 4 of Appendix A. The devices, which are accurate to within .08 per cent, create a potential difference proportional to the table position. This is monitored at the control panels by a pair of meters calibrated to measure displacement in millimeters. An electrical block diagram of the X-Y table is shown in Fig. 4.

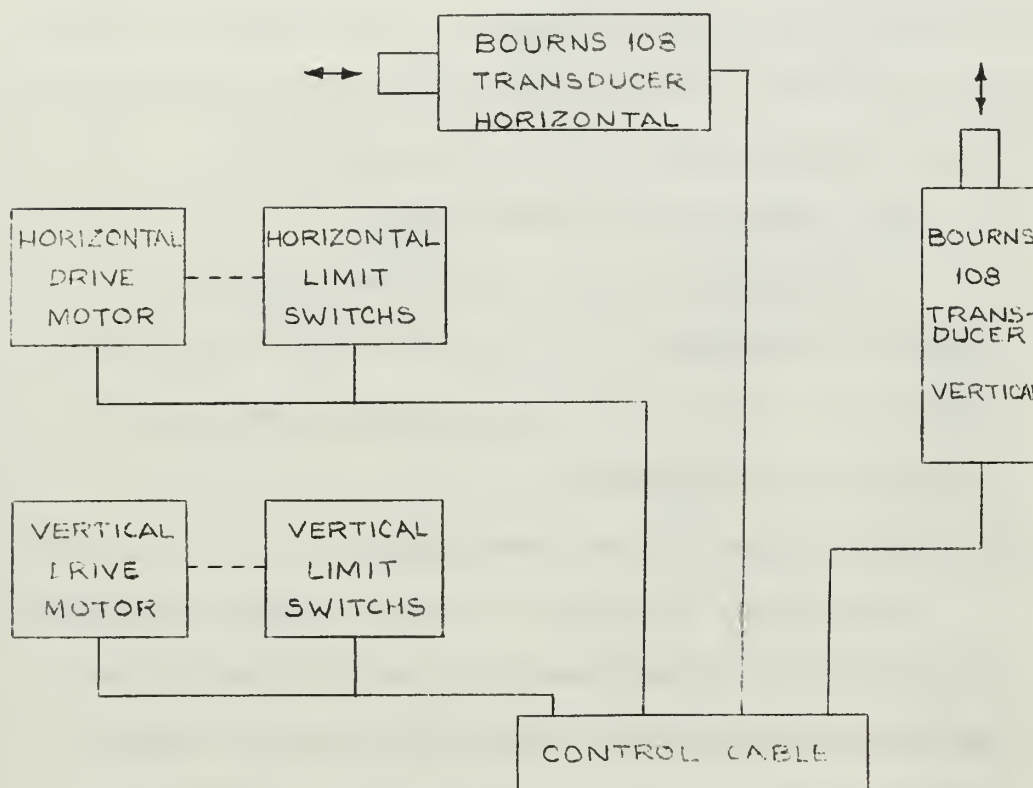


Figure 4. Electrical Block Diagram of X-Y Table

IV. CONTROL STATION APPARATUS

The control panels used for radiation effects experiments are located in a section of the Linac control station separate from the Linac controls themselves. Figure 5 of Appendix A shows the arrangement of the various control modules. From here the wheel assembly is placed correctly, the desired circuit is rotated into position, input signals and potentials are applied, outputs of the circuit are displayed, and beam characteristics are monitored. A detailed description of the components and the manner in which they are used follows. The order of description follows the numbering used in Fig. 6 of Appendix A.

1. HP 721 Hewlett-Packard Power Supply.

This provides either a positive or negative bias between 0 and 30 volts. It is used to bias transistors, integrated circuits, or isolated components of a circuit such as the Fairchild 969.

2. HP 721 Hewlett-Packard Power Supply.

This supply is similar in function to that above except for a modification to provide only positive bias through a BNC panel jack connector. This modification was made in an effort to minimize all possible noise sources. It is used to bias the Fairchild 962 and 969 logic circuits as well as other components.

3. Table Position Indicator.

This panel indicates the horizontal and vertical position of the X-Y table. Two linear potentiometer transducers sense the horizontal and vertical position. The

deflection scale of the meters is regulated by calibrating potentiometers located on the meters is regulated by calibrating potentiometers located on the panel. A wiring diagram of the meters is shown in Fig. 5 and the panel is shown in Fig. 6.

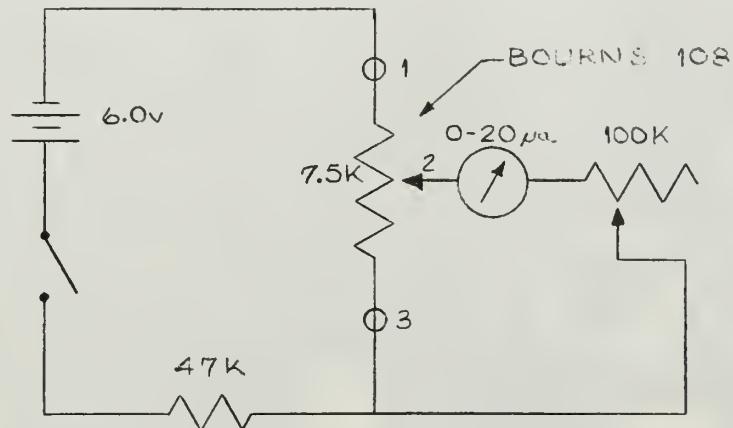


Figure 5. Wiring Schematic of Table Position Indicator

4. End Station Control Panel.

Figure 6 shows this panel in detail. On it are located the controls for table movement, single pulsing, wheel rotation, and relay control.

a. X-Y Table Controls. The "up-down" and "left-right" switches are used to move the X-Y table and in turn the wheel assembly which contains the circuits and the X-Y cross hairs in a plane perpendicular to the beam. This movement places the device under test in the position of maximum beam intensity. Lights by the switches indicate when the table is at its limits,

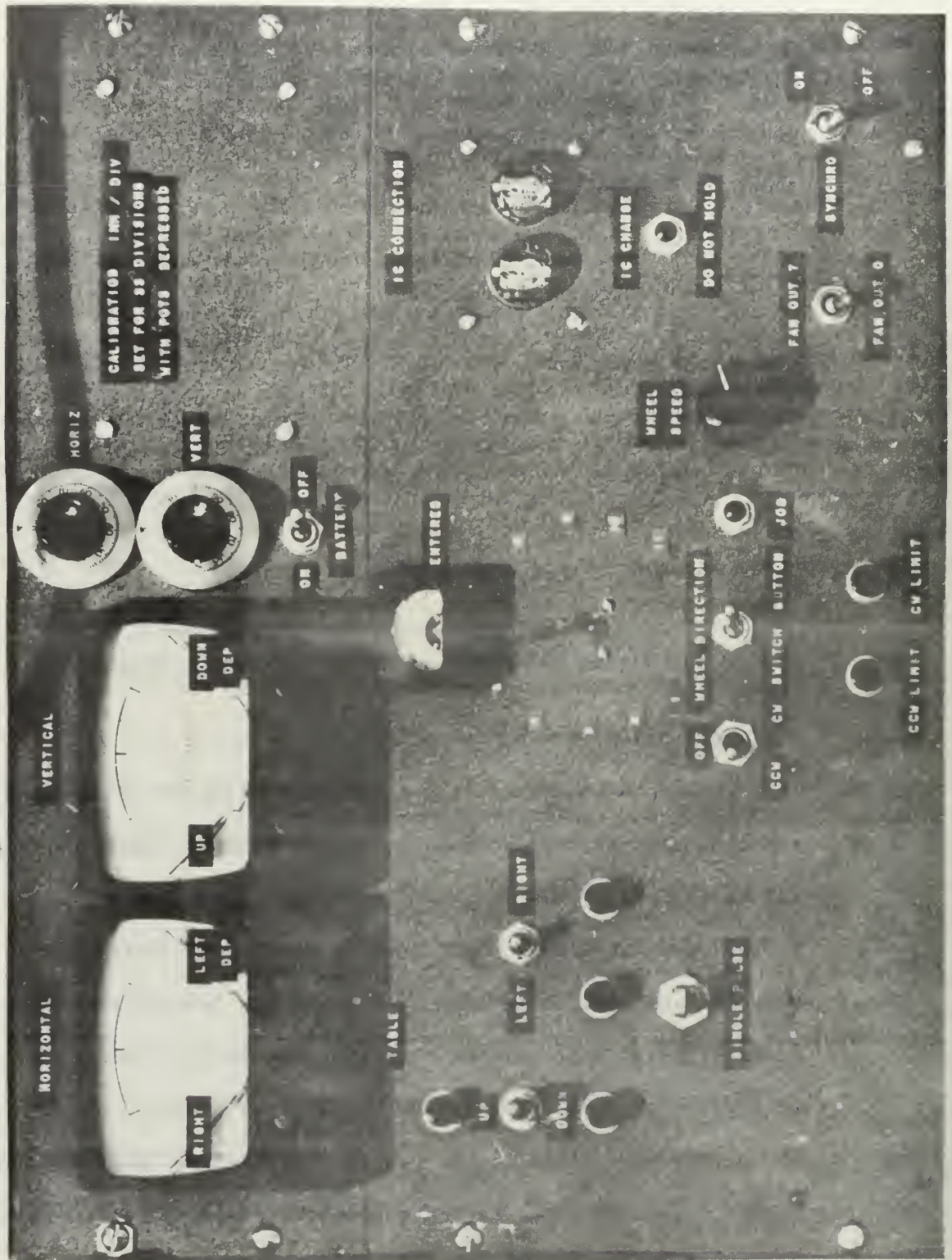


Figure 6. End Station Control Panel

b. Single Pulser. The single pulse or multiple pulse mode of operation is chosen at the Linac main control console. The single pulse switch is energized when in the single mode and allows single pulsing control from this panel.

c. Wheel Positioning. This section is used to rotate the wheel disc in order to position the desired socket in the beam path. There are two modes of rotation; one for rapidly slewing the disc into the vicinity of correct socket position as indicated by a synchro and the other to jog the disc so that the socket is positioned exactly in front of the cross hairs in the beam center. There is a variable speed control for use in the jog mode. When the disc is correctly positioned, a photo cell is activated causing deflection in the centering microammeter. Limit switches allow the disc to be rotated only 320 degrees. Lights reveal that the disc is at its limits.

d. Relay Control. This switch steps the Clare relays located in the wheel assembly. These electrically connect the leads from a given socket to the single set of input-output cables. The two Nixie tubes indicate which socket is connected.

5. Tektronics 556 Dual Beam CRO with 1A1 Plug-in.

This CRO is used for many purposes. The three most important uses, however, are (a) time profile analysis of the beam pulse used for Linac tuning and dosimetry, (b) display of spatial profiles of beam intensity, and (c) measurements of photo currents and other transient effects in reversed biased diodes, transistors and other devices.

6. Wavetek Signal Generator.

This is incorporated in the panel but is not a part of the system at this time.

7. Honeywell Strip Chart Recorder.

This plots input signal against time, and has a maximum sensitivity of 0.1 millivolts full scale. The recorder is used mainly to plot the signal from one of the wheel cross hairs as it is passed through the beam, thus giving a spatial profile of the beam.

8. HP 425A DC Micro Volt-Ammeter.

This meter has a full scale deflection sensitivity of 10 picoamperes. It is used for measuring the dc reverse current characteristics of both forward and reverse biased junctions.

9. Tektronics 503 CRO.

This scope has a calibrated horizontal and vertical sweep with a maximum sensitivity of 1 millivolt per centimeter. This Type of calibration allows one to observe directly the input-output characteristics, the switching parameters, the transfer characteristics, and the dc switching levels of a circuit.

10. Wavetek Signal Generator.

This is used to generate input switching signals for the IC logic circuits. It is also used to generate the horizontal sweep on the 503 CRO when observing transfer characteristics. The signal generator has a multi-function and multi-polarity capability of sine waves, square waves, and sawtooth waves.

V. DOSIMETRY

A. CALCULATED DOSE RATE FROM SECONDARY EMISSION MONITOR READINGS.

A primary indication of Linac tuning is the current measured by a secondary emission monitor, (SEM), which determines beam current by measuring the current of secondary electrons emitted from thin foils. The SEM reliability is questionable except when the beam is closely bunched and passes through its center. If the beam is scattered and sprayed along the walls of the SEM the indicated current increases.

In radiation effects experiments a single SEM is used, located in front of the target chamber which is used in nuclear experiments. After passing through the SEM the beam proceeds through the target chamber, which is sealed by an aluminum window of six mils thickness, and then through 18 inches of air before reaching the integrated circuit. Between the SEM and the target the energy loss is negligible, yet there is appreciable scattering.

In addition to the uncertainties mentioned above, the SEM provides no time resolution of the instantaneous intensity during a pulse, nor any indication of pulse duration. Hence, the SEM fails to show, for example, that the electrons may be spread over twice the pulse duration expected. Similarly, a significant shift in electron density from the leading edge of the pulse to the rear could occur without being detected. If, however, the electron density is constant during the pulse, then the dose rate can be computed from the SEM current as follows:

$$\text{Dose Rate} = (\text{Flux}) \left(\frac{1}{\rho} \frac{dE}{dx} \right)$$

$$\text{where Flux} = \frac{\text{average current}}{(\text{p.r.r.}) (\text{pulse duration}) (dA)}$$

(p.r.r. = pulse repetition rate)

(dA = beam cross sectional area)

The above variables are limited by the capability of the machine.

The Linac pulse duration is varied by altering the length of an open RG-8 cable in the grid pulser circuit. Some increase in the dose rate results from shortening the pulse from 1 μ sec to 0.5 μ sec. Approximately equal numbers of electrons remain in the pulse, thereby producing a higher pulse rate. (This method has been carried to a lower limit of 0.5 microseconds after which arcing was produced in the grid pulsing network).

The beam cross sectional area in the center of the target chamber has been measured to be approximately 0.2 cm². This is discussed subsequently. The value of $\frac{dE}{\rho dx}$ for silicon⁴ at 80 MeV is 1.93 $\frac{\text{MeV cm}^2}{\text{gram}}$, where this value reflects only ionization loss. Radiation loss is not included since the mean free path of the bremsstrahlung photons, in this energy range, is large compared to the thickness of the circuit. With the machine operating at a pulse repetition rate of 60 pulses per second, a pulse duration of 0.5 microseconds, and a typical SEM current of 2.85 microamperes, a dose rate of 1.03 x 10¹¹ rads per second is calculated for silicon.

The circuit is not located at the center of the target chamber, however, and there are two factors which tend to spread the beam and, in turn, lower the dose rate below that computed for the center of the target chamber. First, the quadrupoles are calibrated to focus the beam at the center of the chamber, thus the beam diverges beyond

this point. The proper currents for the quadrupoles which will focus the beam at the location of the circuit have not been determined accurately. Second, the beam is scattered by the 6 mil aluminum window and the 18 inches of air between the target chamber and the circuit. The magnitude of this effect is calculated as follows:

For multiple scattering, the mean projected scattering angle, θ_{mp} , is given by⁵

$$\theta_{mp} = \frac{12 \text{ (MeV)}}{pv \text{ (MeV)}} \frac{(\text{length in medium})^{\frac{1}{2}}}{(\text{radiation length})^{\frac{1}{2}}} (1 + \epsilon),$$

where ϵ is a correction factor for the Moliere Theory upon which this expression is based. This factor is a function of electron velocity and the thickness of the target. The calculated values of θ_{mp} for the window and the air are 3.9×10^{-3} radians and 3.7×10^{-3} radians respectively.

Assuming that a parallel beam strikes the window, a mean projected displacement of 3.5 mm will occur at the location of the circuit. This dispersed beam spot causes a decrease in the dose rate by a factor of six from that computed above. Since the beam striking the window is not necessarily parallel any divergence of the beam by the quadrupoles will lower the dose rate even more.

B. X-Y CROSS HAIRS.

The X-Y cross hairs, discussed in connection with the wheel design, are used to give profiles of beam intensity as a function of coordinate position or as a function of time. As the beam passes through the cross hair wires it causes secondary emission of electrons

and thus a positive potential on the wires. When a 50 ohm termination is used to match the cable impedance, a frequency response is produced which is adequate to display a pulse profile on the Tektronics 556 dual beam CRO. Without termination the response time is 30 milliseconds. The unterminated line stores charge and thereby enables the Honeywell recorder with its slow response time to plot average intensity. Initial experiments indicate that the amplitude of the potential is directly proportional to the beam intensity as measured by the SEM. The wire used for the cross hairs was nichrome 29 gauge.

A similar effect would occur if the wires acted as probes in a field of positive ions. To measure the effect that ionized air might contribute, a set of cross hairs identical to those in the wheel assembly was placed in the target chamber. Mini-coaxial cable shielded the wires connecting the cross hairs to BNC connectors at the bottom of the target chamber. The amplitude of the signal from the cross hairs in the target chamber was compared to that in the wheel assembly at atmospheric pressure and at various pressures down to 160 microns. The amplitude in air appeared to be slightly greater than in vacuum but, in general, there were no significant differences. Thus, the main contribution to the potential is apparently secondary emission.

The point of maximum intensity in the electron beam can be determined by moving the cross hairs horizontally and vertically with the X-Y table until the signals from both wires are maximum. Figure 7 shows two profiles obtained in this way.

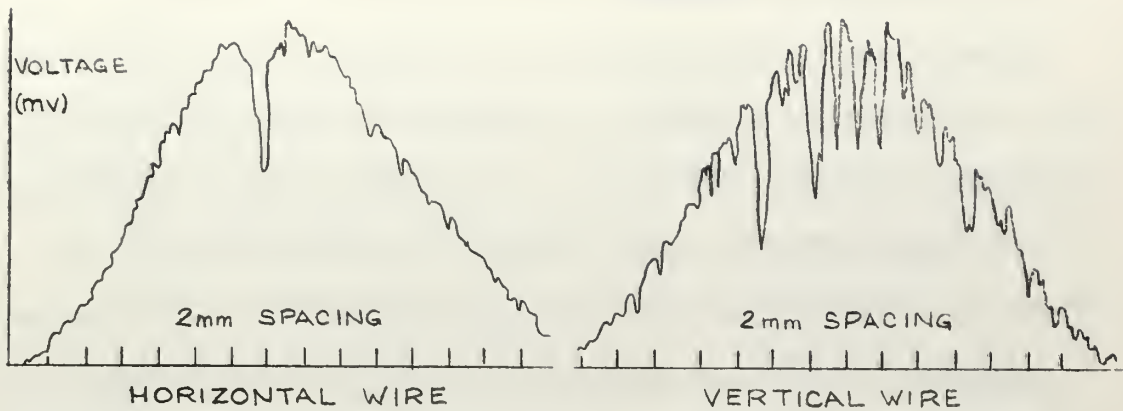


Figure 7. Integrated Current Profiles

These are not true profiles of intensity, but rather of integrated current taken by maximizing the intensity on one wire and passing the other wire through the beam. The similarity of the two profiles, one taken in the horizontal direction and the other in the vertical, indicates that the beam is approximately symmetrical about its center.

The instantaneous electron flux can change between the leading and trailing edge of the pulse. By placing the cross hairs in the center of the beam and displaying the signal on the Tektronics 556 CRO the time distribution of the pulse is observed. The frequency response of the system is adequate to show variations in intensity of duration as short as about 10 nanoseconds. When the Linac is carefully tuned the intensity goes to a maximum quickly and remains at a constant plateau until the rapid decay at the trailing edge of the pulse. A collection of time profiles is discussed in section VI.

C. COLOR FILM DOSIMETERS

Dyed color films manufactured for theoretical lighting have been investigated as dosimeters in the megarad range by the Naval Radiological Defense Laboratory⁶. The parameter used as a measure of dose is the change in optical density or, alternately, the change in transmission of the film. From experiments done with 61 different films NRDL concluded that a particular color, Number 48 "bright rose",* encompassed the broadest range of dose response, extending from 2.5×10^5 to 5×10^7 R, and had the greatest sensitivity.

Samples of bright rose film have been irradiated in the target chamber, outside of the target chamber at the rear window, and at the wheel assembly. In all cases it was found that the beam intensity was symmetric about the center. Appendix B shows plots of dose versus position for the various exposures. Each curve has been normalized to give the same area, i.e., the same total dose.

TABLE I
DIAMETERS OF BEAM INTENSITY

<u>Position</u>	<u>1/4 Intensity</u>	<u>1/2 Intensity</u>	<u>3/4 Intensity</u>
Target Chamber	7	5	4.2
Rear Window	12	8	4.5
Wheel Assembly	10.5	11.5	7.5

*Manufactured by Strand Electric and Engineering Co., Ltd., London, England. Distributed by Kliegl Bros., New York, N. Y.

Table 1 gives data concerning the beam diameter and cross sectional area at the three locations. It was from this data that the area of one-half intensity for the beam in the target chamber was computed and used in a previous section to determine the dose rate.

The ratio of the cross sectional beam area at the target chamber to that at the wheel assembly (using the radius of one-half intensity) is the factor by which the dose rate is decreased. From the data in Table 1 this ratio is .17, which predicts a rate of 1.8×10^{10} rads per second at the wheel assembly.

The scattering as computed earlier added to the dimensions of the beam at the target chamber and gave a diameter of 1.18 cm. This compares favorably with the measured diameter of 1.15 cm.

VI. TUNING THE LINAC USING TIME PROFILES OF BEAM PULSES.

The time profiles of beam pulses indicated by the cross hairs described earlier provide sensitive and potentially very useful indications of the state of Linac tuning. A series of drawings from photographs of time profiles taken under various conditions of Linac tuning and deliberate mistuning follows. In each of the figures below the upper trace represents the signal from the vertical wire and the lower trace that from the horizontal wire.

The ideal profile should approach a square pulse of duration determined by the length of the pulse which allows injection of electrons into the accelerating sections. Figure 8 shows a display from the cross hairs with the Linac under best tuned conditions and shows the approximate square form.

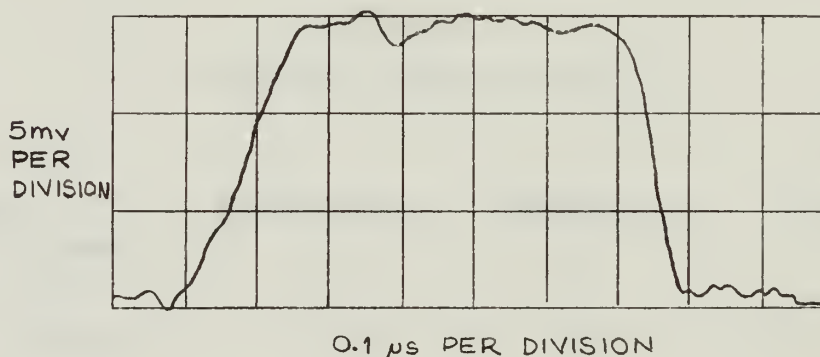


Figure 8. Time Profile of Correctly Tuned Beam

Linac frequency is one of the most critical parameters in maintaining a uniform pulse. As frequency is changed, a dip occurs in the middle of the pulse. The pulse is separated into two peaks

with the second peak (in time) diminishing more quickly if the frequency is driven too high and the first peak if the frequency is driven too low. Figure 9 shows a sequence of profiles as the

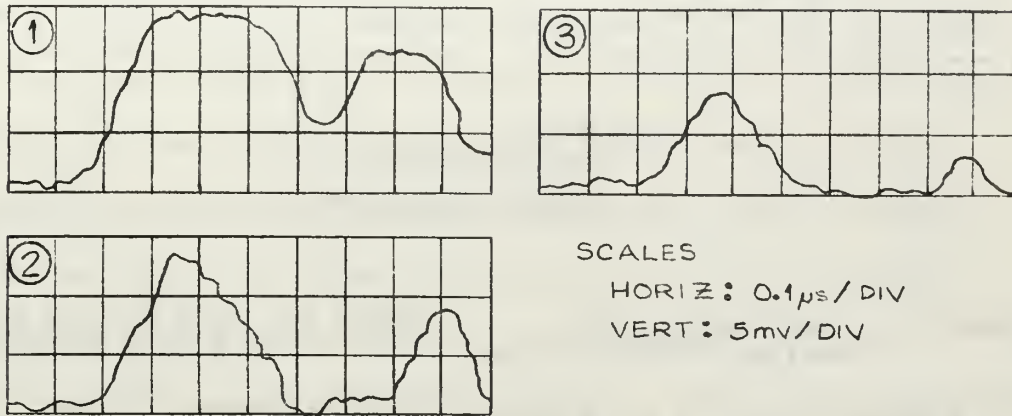
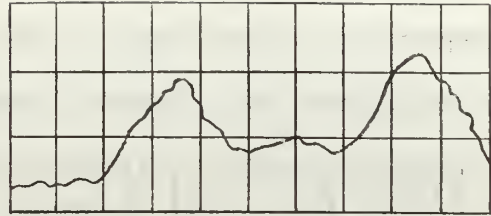
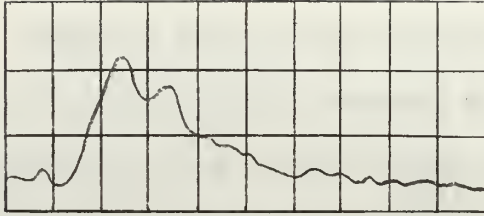


Figure 9. Sequence of Time Profiles as Frequency is Raised

frequency is raised from the tuned position. Conditions have been observed in which the frequency was incorrect, producing two peaks separated by as much as 0.2 microseconds, yet giving the same SEM current as did the beam when bestuned. Hence, tuning the Linac by using the maximum SEM current does not necessarily guarantee the best pulse.

The effects of poor phasing are more subtle and less consistent. In general, if phasing of the third accelerator section is late relative to sections one and two, a decrease in amplitude as observed, decreasing more rapidly in the latter part of the pulse. This is displayed in Fig. 10. When the third section phasing is too early, as in Fig. 11, a decrease in amplitude at the front of the pulse is observed but also seen is a pulse splitting effect, as if the frequency were changed. This points out the interrelationship between most Linac tuning parameters.



SCALES

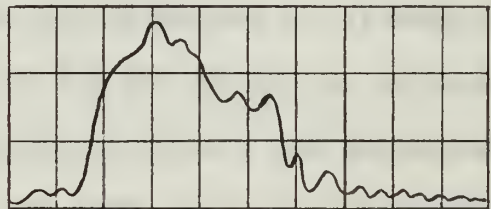
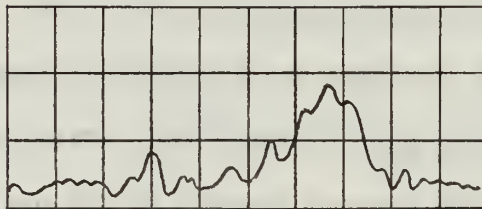
HORIZ: $0.1 \mu\text{s} / \text{DIV}$

VERT: $5 \text{ mV} / \text{DIV}$

Figure 10. Time Profile with Section 3 Phasing Late.

Figure 11. Time Profile with Section 3 Phasing Early.

Without the use of the quadrupole magnets a change in the current of the deflection magnets moves the beam horizontally and leaves only the outer energy fringe directed toward the target. Considerable pulse to pulse variation occurs in fringe energy giving the intensity spread seen in Figs. 12 and 13. The leading edge of the pulse decays first if the deflection magnet current is too high; the lagging edge if the current is too low.



SCALES

HORIZ: $0.1 \mu\text{s} / \text{DIV}$

VERT: $5 \text{ mV} / \text{DIV}$

Figure 12. Time Profile with Deflection Magnet Current High.

Figure 13. Time Profile with Deflection Magnet Current Low.

There are numerous pulse deformations that are produced by changes in the timing of the gun grid pulse, gun injector pulse, and the driver pulse. Generally, the timing changes produce pulse to pulse fluctuations and a decay in beam amplitude.

One such deformation is of particular interest. Simultaneous changes in driver timing and grid pulse timing leaving all other parameters tuned, diminish the pulse width and slightly increase the pulse intensity. On one observation the grid pulse network was adjusted for a pulse width of 0.5 microseconds, giving a best-tuned SEM current of 2.85 microamperes. The timing modifications were made reducing the pulse width to .1 microseconds and the SEM current to .66 microamperes. This represented a dose rate gain of 1.2 and gave a pulse of the duration necessary to view actual transient photo effects in the integrated circuit. Figure 8 represents the pulse on which changes were made and Fig. 14 shows the .1 microsecond pulse. Note the slight increase in amplitude in the narrow pulse showing the intensity correlation between the SEM and the cross hairs.

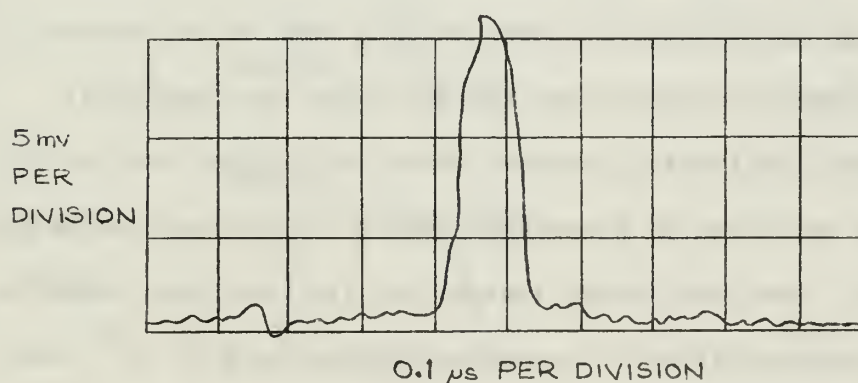


Figure 14. Time Profile of 0.1 Microsecond Pulse

VII. RADIATION EFFECTS EXPERIMENTS

The experimental data from NPN and PNP transistors, field effect transistors, NPN transistors isolated from a logic circuit, and the outputs of an IC logic circuit are presented in this section.

Various transistors were exposed and the transient responses recorded. The two circuit configurations used for these exposures are shown in Fig. 15. Both circuits were reverse-biased with the

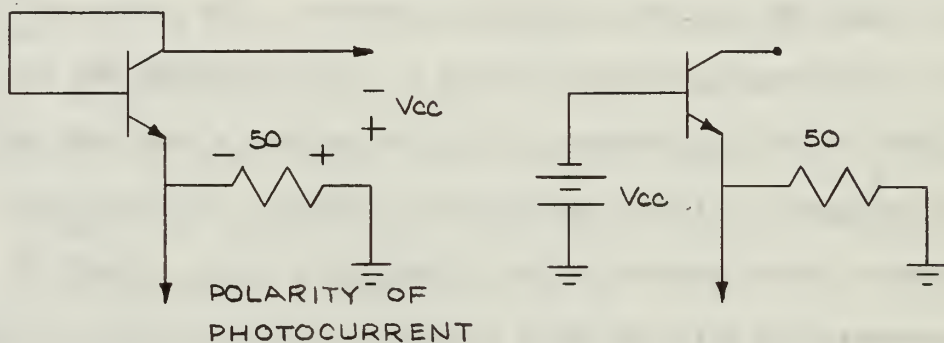
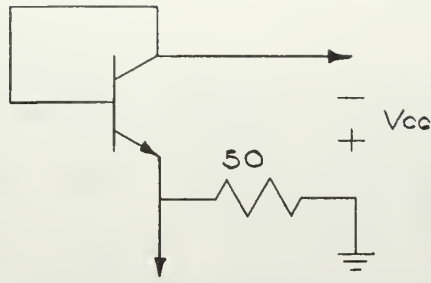


Figure 15. Circuit Configurations for Exposing Transistors

magnitude of these biases adjustable. The resulting waveforms are shown in Table 2. Note that not all variations of V_{cc} were checked; only a confirmation of values was desired. Accurate dosimetry was not attempted. Note further that at the time of these measurements (made before the X-Y table was completed) the necessary positioning accuracy which would place the circuit in the beam could not be guaranteed, hence, the values are only approximate. Even with these limitations the waveforms compared with the expected values at an estimated dose rate of 10^{10} rads per second. These results established the adequacy of the

CONFIGURATION



WAVEFORMS

$\frac{1}{2} \mu s$ BEAM PULSE WIDTH
 TIME SCALE $\frac{1}{2} IN. = 1 \mu s$

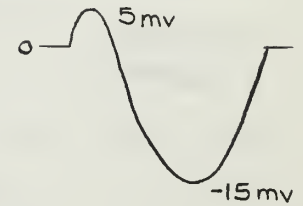
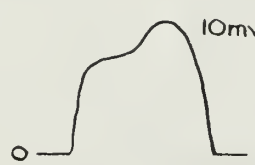
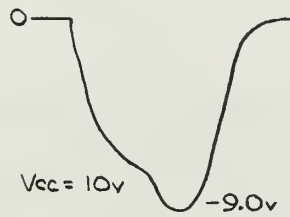
TRANSISTOR

REVERSE BIAS

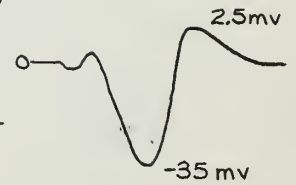
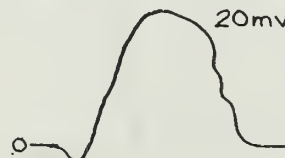
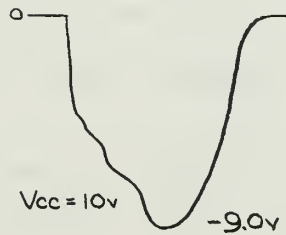
$V_{cc} = OPEN$

$V_{cc} = 0$

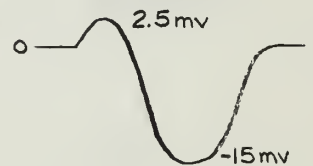
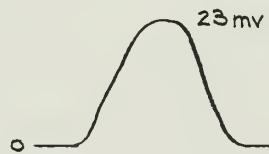
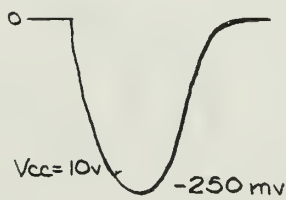
2N1304
 TEXAS
 INSTRUMENT
 NPN



2N1304
 TEXAS
 INSTRUMENT
 NPN
 WITHOUT
 METAL CAN



2N736
 NPN



2N535B
 PNP

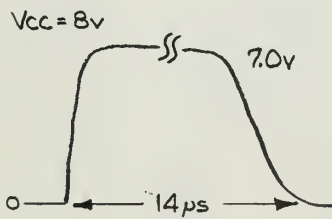
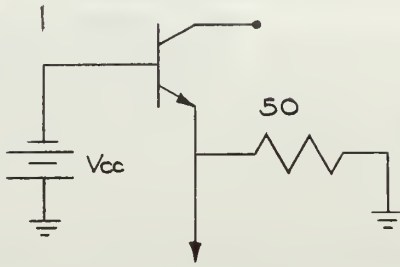


TABLE II

CONFIGURATION



TRANSISTOR	REVERSE BIAS	$V_{cc} = \text{OPEN}$	$V_{cc} = 0$
2N1304 WITH CAP	 $V_{cc} = 6$ -4.4v	 15mv -5mv	 -80mv
2N736	 $V_{cc} = 6$ -150mv		 -30mv
2N535B		 50mv	 270mv 5µs

TABLE II (continued)

measuring apparatus and allowed the research to proceed to testing of isolated integrated circuit components and logic circuits with some hope of success.

In a separate project⁷, similar tests on field effect transistors, which used the wheel assembly and the same monitoring equipment, were conducted. The results agree with those published in other papers and again demonstrate the reliability and adequacy of the wheel assembly and associated monitoring equipment.

Later, tests were made which were similar to those conducted previously but now employed the X-Y table, which allowed positioning accuracy to within 0.2 mm. Isolated transistor components from a conventional Fairchild DTuL 969 logic circuit were irradiated. The circuit configurations and the resulting waveforms are shown in Fig. 16. One of the configurations (Fig. 16a) was used in the

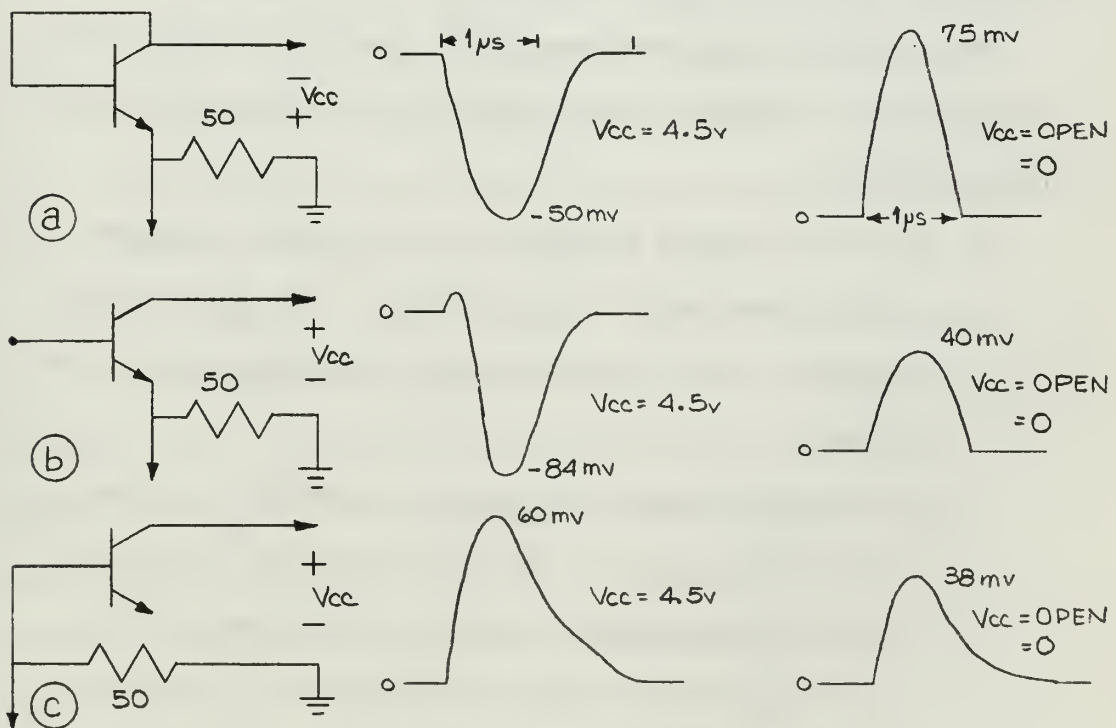


Figure 16. Isolated Component Circuit Configurations and Waveforms

transistor tests discussed above and was used by Fairchild to produce a diode within an integrated circuit. The $V_{cc} = 0$ conditions were achieved by shorting the bias cable in the control station area. To evaluate the contribution made by the socket, the integrated circuit was removed and the experiment was repeated using the configuration in Fig. 16b. A positive 8.0 mv signal was obtained which varied only slightly with changes in the bias from -30 to 30 volts. Such peripheral effects caused by instrumentation response, package response, and charge scattering are closely documented in a report by Long and Baer³. When a reverse bias was placed on the respective diode configuration each of the waveforms compared favorably with data published in other reports. When the radiation parameters of the isolated component are known insight can be gained into the entire logic circuit which may contain 10 or more active devices.

Observation of the waveforms of the junction transistor and of the isolated component of the logic circuit, presented several points as noted:

- a. The photo current observed in the isolated component was smaller than that in the transistor. The photo current appeared to vary in proportion to the dimensions of the device.
- b. The package response had polarity reversed in comparison to the photo current. The package area of the dual in-line 969 that was perpendicular to the beam was much larger than the package of the conventional transistor, and thus gave a larger response. The factors that make

up this response are indeed complex and can include the type of encapsulating material, and the number of external leads and their sizes. In general, the larger the package the greater the expected response.

- c. The polarity of the package response agreed with that of the X-Y cross hairs. The magnitude of the package response was greater than the cross hairs, which was attributed to the larger size of the package intercepting the beam.
- d. The magnitude of photo current was proportional to the dose rate. This was observed by accurately positioning the device and comparing the change in photo current with the change in position.
- e. The direction of the observed photo current was into the N type material as theory would show. One configuration, a base-emitter diode, required a reverse bias of 6.0 volts before a photo current was observed. The device was probably approaching its Zener breakdown which may have contributed to the observed current.

A final experiment was to expose a Fairchild DTuL 969 logic circuit and determine if exposure would cause the device to change its logic state. The 969 is a triple NAND gate circuit with three inputs to each gate. Only one gate was used, with its output connected through a switch to the F.0.7 circuitry, discussed below. Both the output of the F.0.7 circuit were monitored through emitter follower circuits. Two of the inputs to the circuit were connected to Vcc and the other to ground. Figure 17 illustrates this experimental setup.

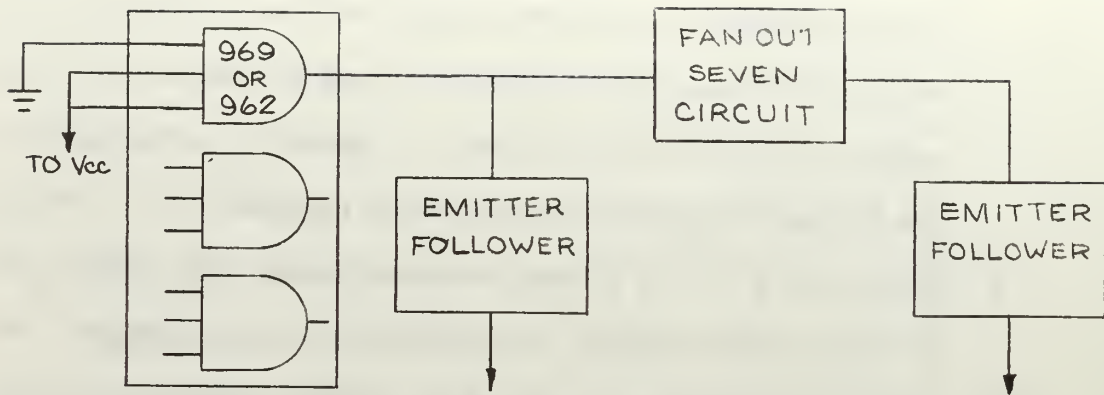


Figure 17. Block Wiring Diagram for Logic State Experiment

The discussed input connections placed the logic circuit in the "on" state with the output at V_{cc} . Theoretical studies indicate that if the device is exposed to a dose rate sufficiently high to cause a change of state, the output from the logic circuit may drop below the value of V_{cc} ; nearly to zero. The recovery time of the device is approximately the same as the electron pulse width when the width is 0.5 microseconds or greater.

Without the emitter followers connected, the response output of the logic circuit was a series of negative pulses below the V_{cc} level. The pulses, shown in Fig. 18, decay exponentially with a time constant depending on the output impedance of the logic circuit, monitoring equipment, and the capacitance of the triaxial cable extending from the device to the monitoring station. This time constant was measured to be 6 microseconds.

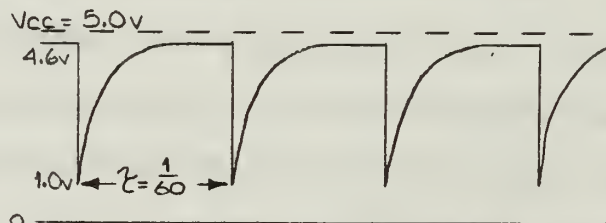


Figure 18. Logic Circuit Output Without Emitter Follower

When the emitter follower circuits were inserted the long exponential tail was eliminated and a response such as that shown in Fig. 19 was recorded. The results show a change in output level of approximately 1 volt when exposed to radiation. It is not known whether this change in level is sufficient to create a shift in the succeeding circuitry and thus, circuit failure. Evidence indicates however, that the present dose rate causes a substantial level change.

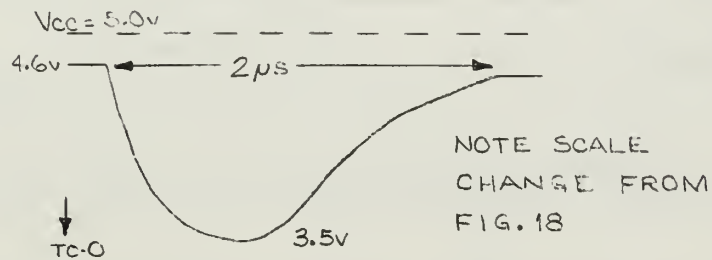


Figure 19. Logic Circuit Output with Emitter Follower

The integrated circuits employed in this research are extremely durable devices. Many have withstood radiation doses that would have easily destroyed other transistors.

F.0.7 CIRCUIT

The F.0.7 circuit can be connected to any one of the three logic gate outputs. It uses a Fairchild DTuL 962 logic circuit with seven of the nine input gates connected in parallel. When attached to the output of a logic circuit, the F.0.7 circuit causes a humping in the curve as given in the Fairchild specifications. The reason for this humping is not known. The transfer characteristic for a given logic circuit with $V_{CC} = 5.0$ volts appears in Fig. 20.

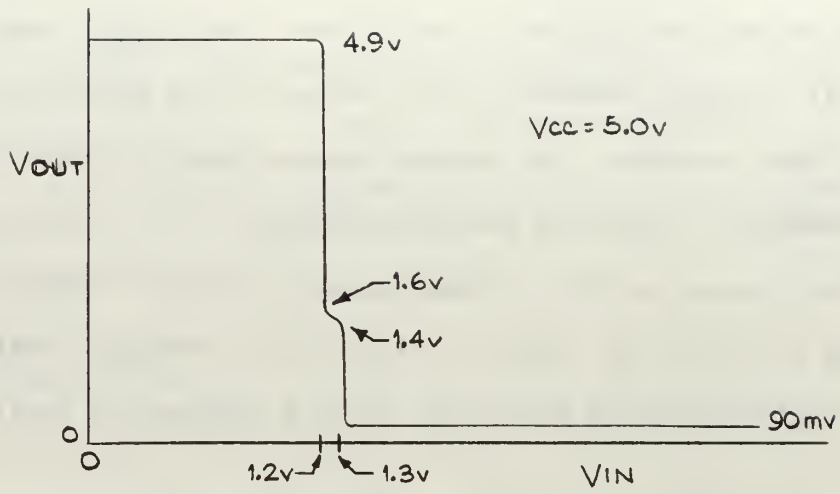
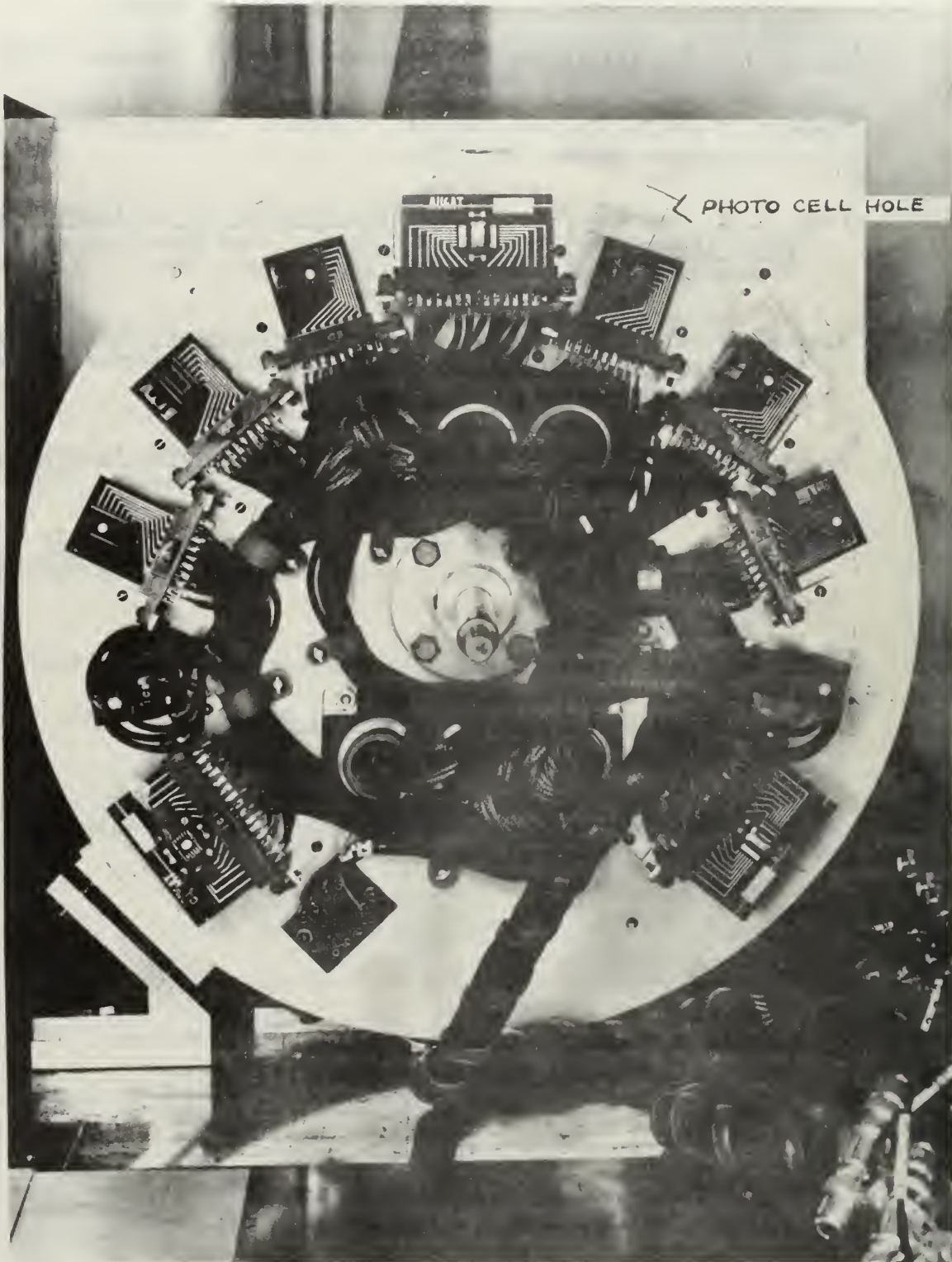


Figure 20. Transfer Characteristics of a Logic Circuit

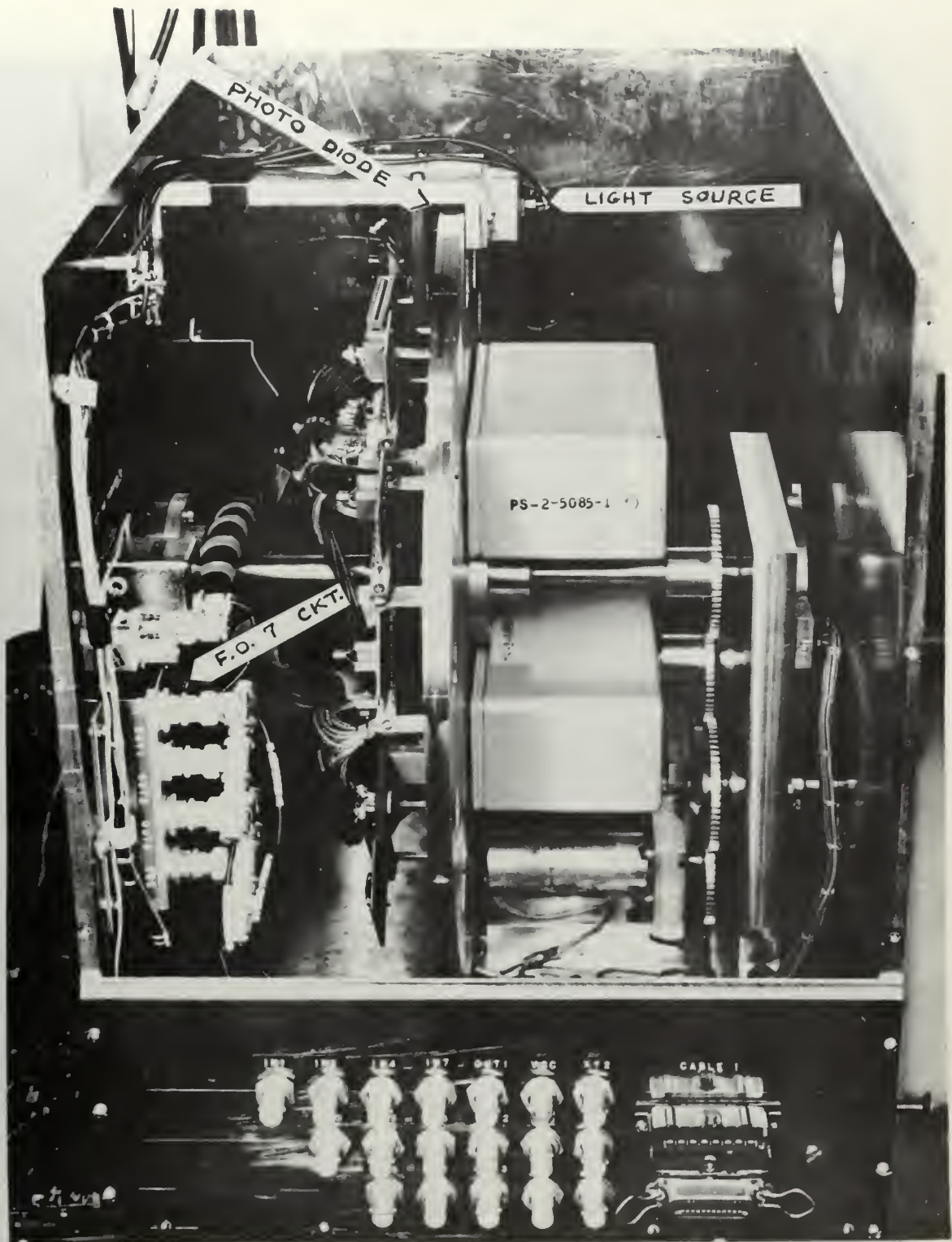
BIBLIOGRAPHY

- ¹Brady, John B., Thesis, Naval Postgraduate School, September 1967.
- ²Barnett, Miles T. Jr., and Cunneen, William J., Thesis, Naval Postgraduate School, May 1966.
- ³Long, D. M., and Baer, R. D., Radiation Effects on Insulated Gate Field Effect (MOS) Integrated Circuits, Army Electronics Command, Fort Monmouth, New Jersey, December 1967.
- ⁴Berger, Martin J., and Seltzer, Stephen M., Tables of Energy Losses and Ranges of Electrons and Positrons, National Aeronautics and Space Administration, Washington, 1964.
- ⁵Barkas, Walter H., and Rosenfield, Arthur H., Data for Elementary-Particle Physics, University of California, Berkeley, 1961.
- ⁶Menkes, C. K., and Goldstein, Norman, Color Films for Megarad Dosimetry, Naval Radiological Defense Laboratory, San Francisco, 1966.
- ⁷Olson, Philip R., Thesis, Naval Postgraduate School, June 1968.
Transient-Radiation Effects on Electronics Handbook, Battelle Memorial Institute, August 1967.
- Raymond, J. P., and Johnson, R. E., Generalized Model for Semiconductor Radiation Response Prediction, Army Electronics Command, Fort Monmouth, New Jersey, 1967.



APPENDIX A

Figure 1. Wheel Disc



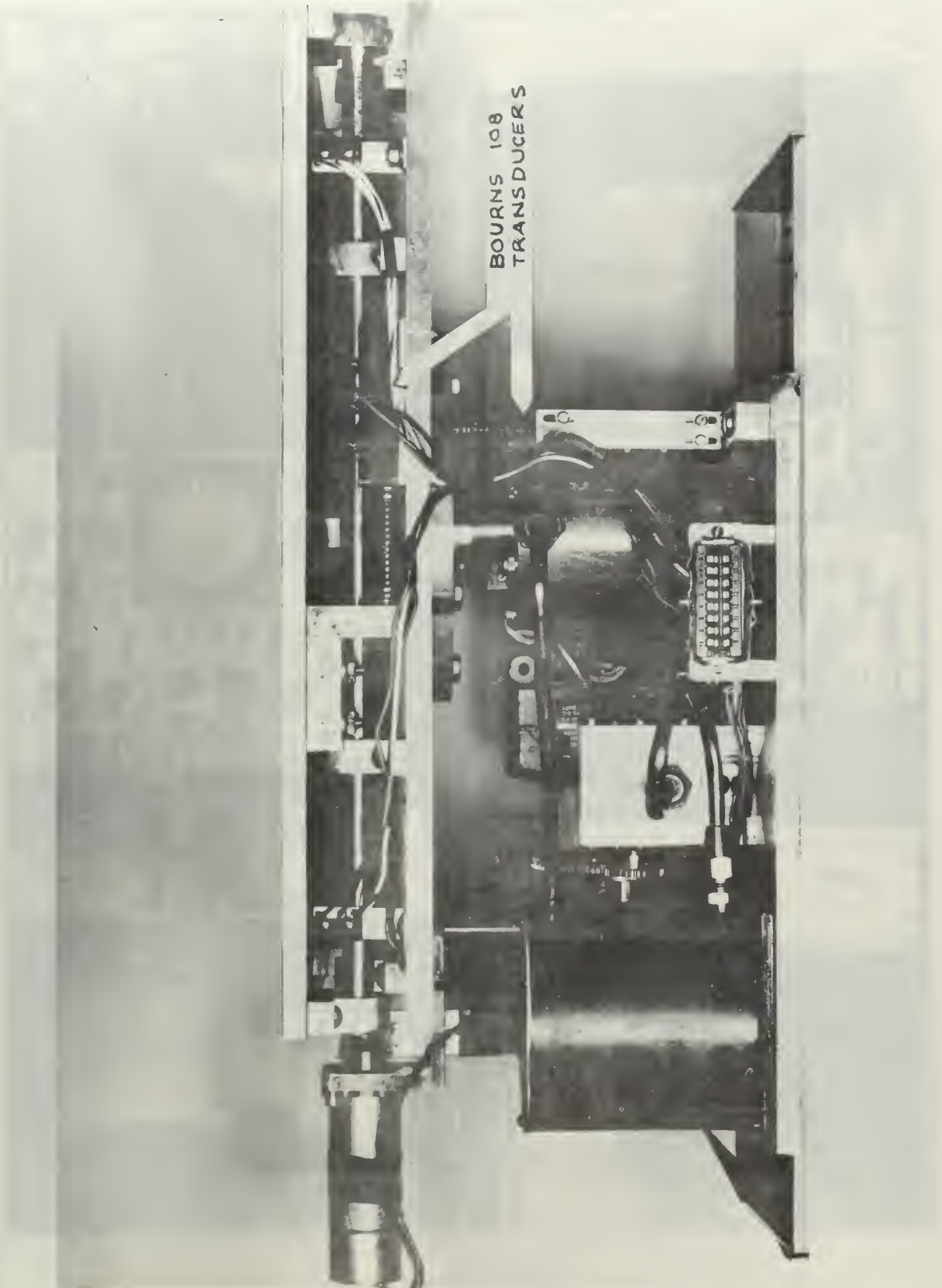
APPENDIX A

Figure 2. Wheel Assembly



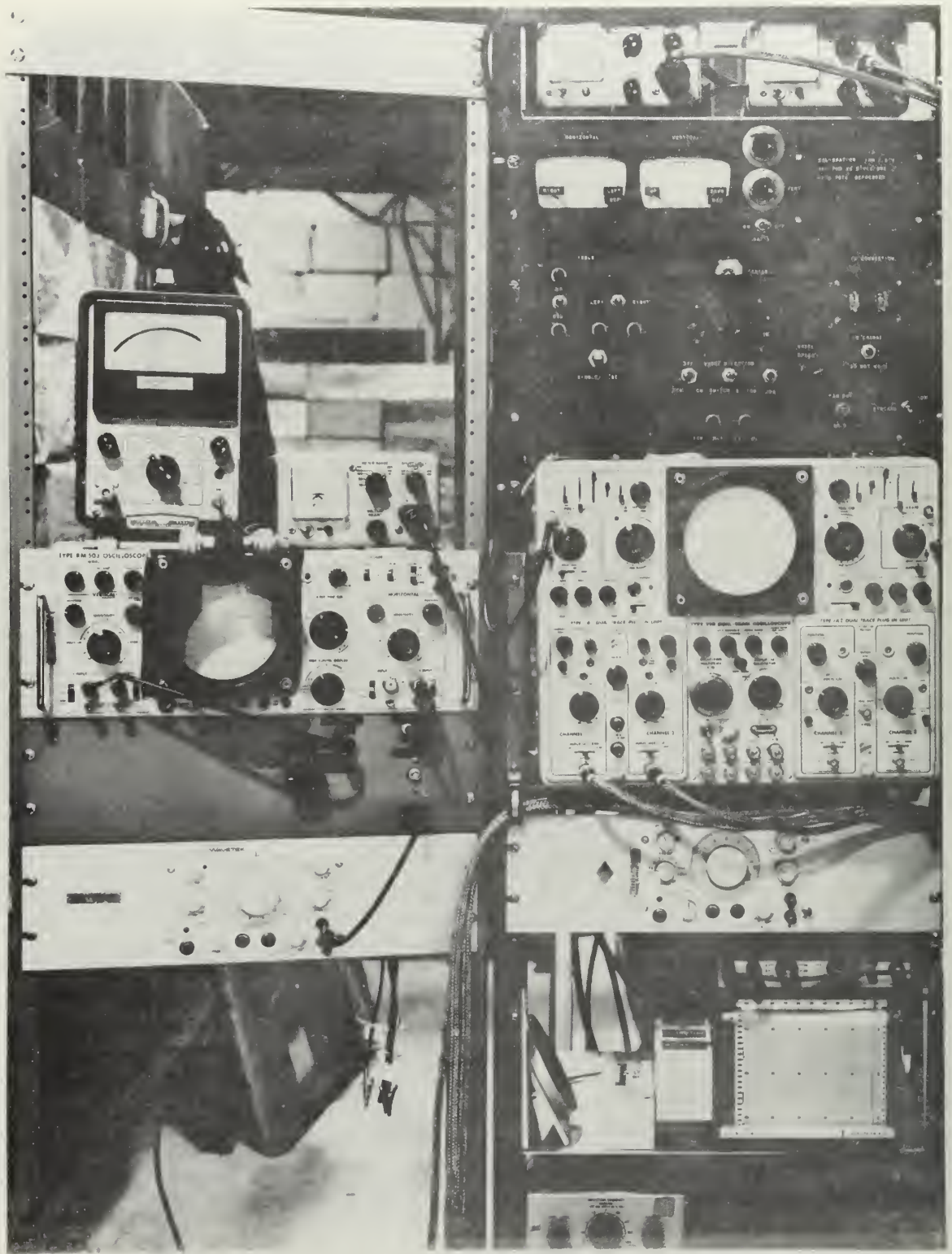
APPENDIX A

Figure 3. Wheel Assembly Showing X-Y Cross Hairs



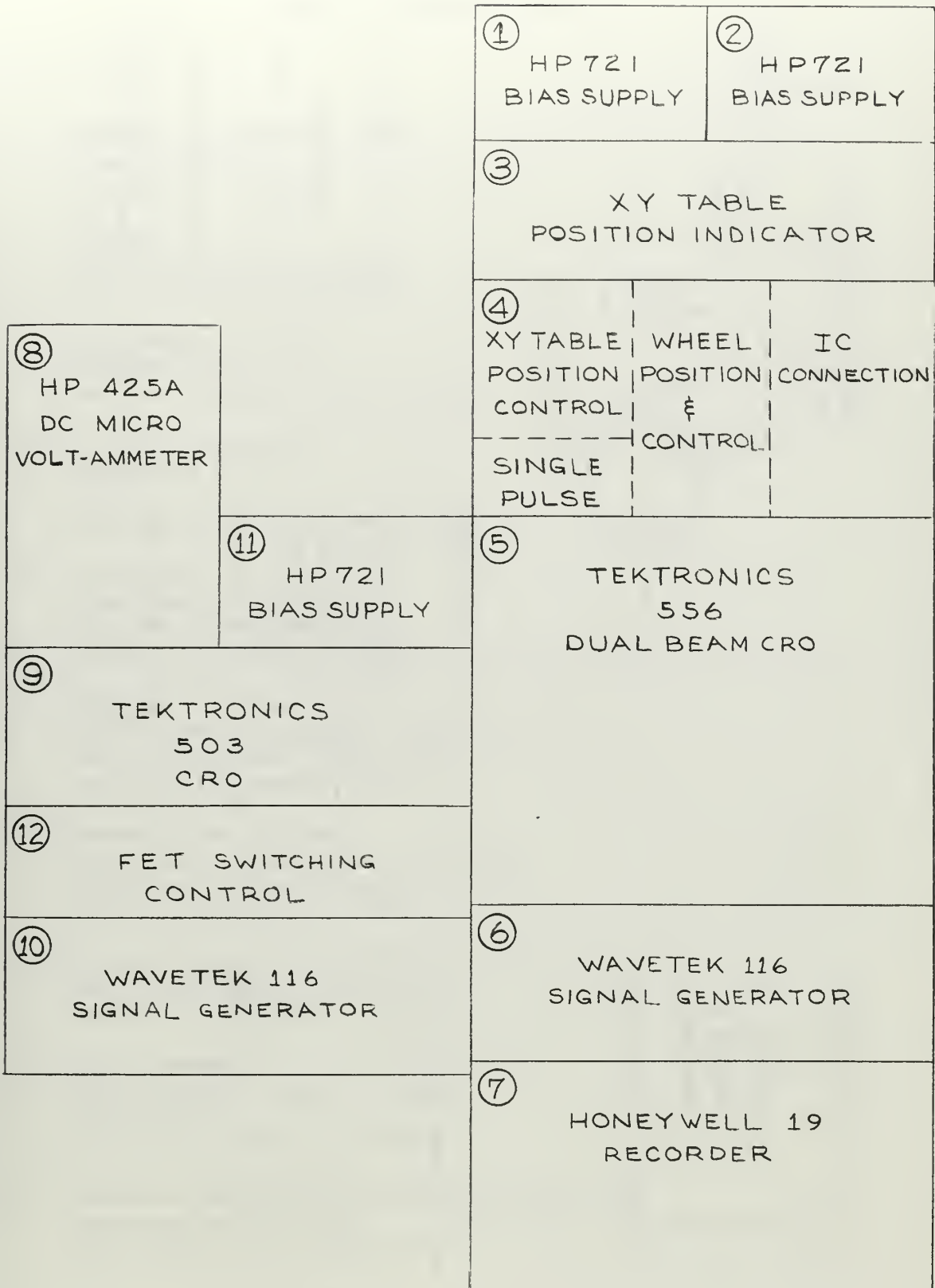
APPENDIX A

Figure 4. X-Y Table



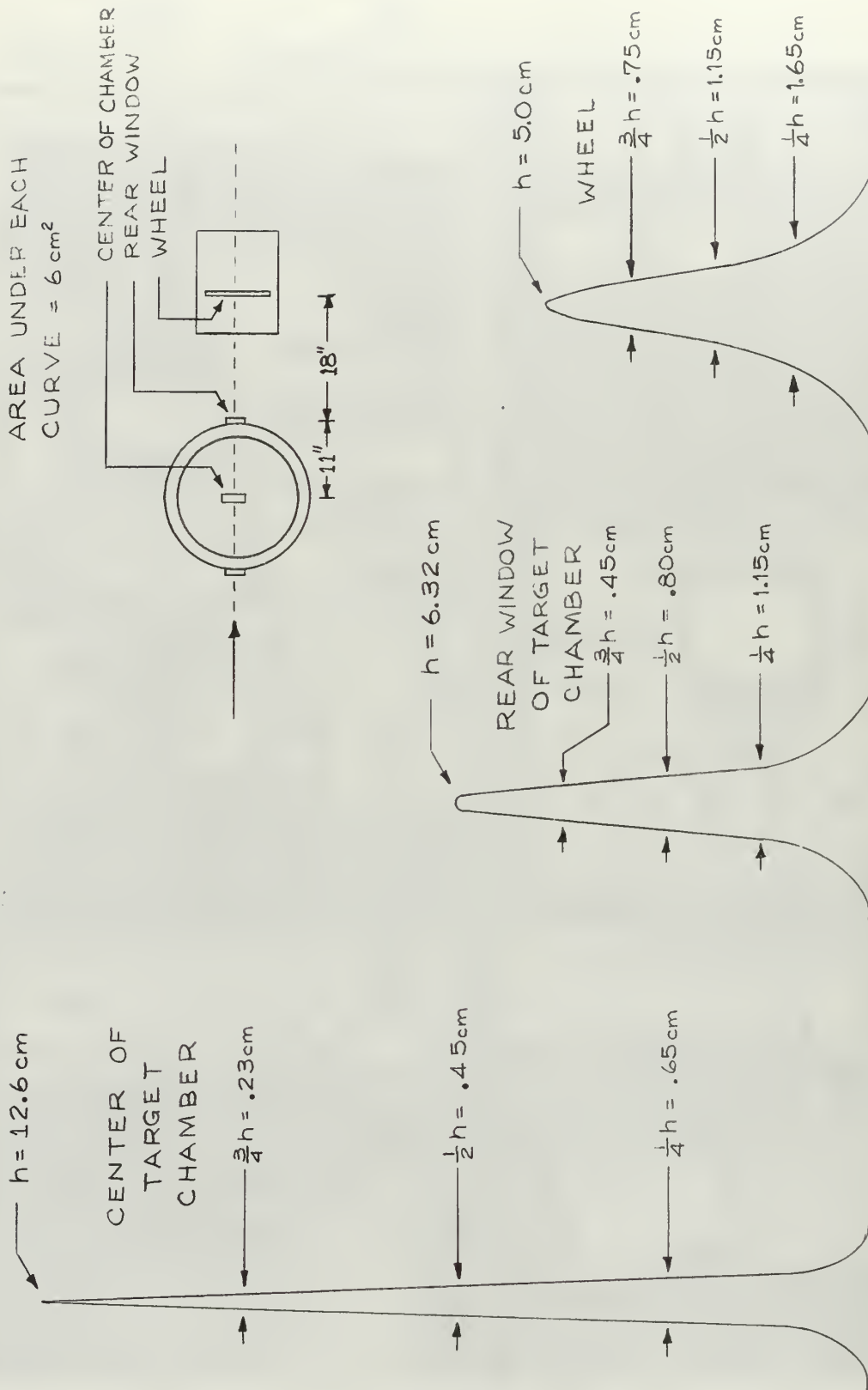
APPENDIX A

Figure 5. Control Panels



APPENDIX A

Figure 6. Diagram Identifying Control Panel Components



APPENDIX B

Figure 1. Color Film Dosimeters

INITIAL DISTRIBUTION LIST

	No. Copies
1. Defense Documentation Center Cameron Station Alexandria, Virginia	20
2. Library Naval Postgraduate School Monterey, California 93940	2
3. LCDR Richard E. Slye USS MAHAN (DLG-11) FPO San Francisco, Calif. 96601	2
4. LT William C. Stark COMSERVPAC Staff Box 22 FPO San Francisco, Calif. 96610	2
5. Professor J. N. Dyer Department of Physics Naval Postgraduate School Monterey, California 93940	10
6. Professor William Brenner Department of Electrical Engineering Naval Postgraduate School Monterey, California 93940	1
7. Professor Shu-gar Chan Department of Electrical Engineering Naval Postgraduate School Monterey, California 93940	1
8. Linear Accelerator Facility Naval Postgraduate School Monterey, California 93940	3
9. Field Command Defense Atomic Support Activity Sandia Base Albuquerque, New Mexico 87100	1
10. Commander, Naval Ordnance System Command Hqs. Department of the Navy Washington, D. C. 20360	1
11. Professor J. R. Neighbours Department of Physics Naval Postgraduate School Monterey, California 93940	1

12. Defense Atomic Support Agency
Department of Defense
Washington, D. C. 20301

1

DOCUMENT CONTROL DATA - R & D

(Security classification of title, body of abstract and indexing annotation must be entered when the overall report is classified)

1. ORIGINATING ACTIVITY (Corporate author) Naval Postgraduate School Monterey, California 93940		2a. REPORT SECURITY CLASSIFICATION Unclassified	
		2b. GROUP	
3. REPORT TITLE A Facility for Transient Radiation Effects Experiments at the NPS Linear Accelerator			
4. DESCRIPTIVE NOTES (Type of report and inclusive dates) Master's Thesis, June 1968			
5. AUTHOR(S) (First name, middle initial, last name) Richard E. Slye William C. Stark			
6. REPORT DATE June 1968	7a. TOTAL NO. OF PAGES 55	7b. NO. OF REFS 9	
8a. CONTRACT OR GRANT NO.	9a. ORIGINATOR'S REPORT NUMBER(S)		
b. PROJECT NO.			
c.	9b. OTHER REPORT NO(S) (Any other numbers that may be assigned this report)		
d. Unlimited distribution			
10. DISTRIBUTION STATEMENT This document is subject to special export controls and each transmittal to foreign government or foreign nationals may be made only with prior approval of the Naval Postgraduate School.			
11. SUPPLEMENTARY NOTES		12. SPONSORING MILITARY ACTIVITY Naval Postgraduate School Monterey, California 93940	
13. ABSTRACT Mechanical hardware has been developed that remotely places integrated circuits, transistors, and other fixed components into an electron beam in a manner which allows measurements of radiation effects. The associated circuitry used for these measurements is presented, as well as the methods employed in reducing RF noise. A technique which uses a set of cross hairs to give time and spatial beam profiles which aid linear accelerator tuning and beam manipulation is described. Initial transient radiation effects experiments have been conducted and photo currents observed. Schematics, pictures, and construction details of the apparatus are presented.			

14.

KEY WORDS

LINK A

LINK B

LINK C

ROLE

WT

ROLE

WT

ROLE

WT

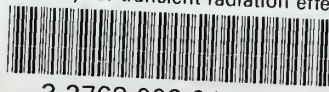
Linear Accelerator
Electron Radiation Effects



NO. 1001

thesS5718

A facility for transient radiation effec



3 2768 002 01162 9

DUDLEY KNOX LIBRARY